Applied Thermal Engineering 31 (2011) 803–810

Contents lists available at ScienceDirect

Applied Thermal Engineering

journal homepage: www.elsevier.com/locate/apthermeng

# Optimizing the geometrical parameters of a spark ignition engine: Simulation and theoretical tools

P.L. Curto-Risso [a], A. Medina [b,*], A. Calvo Hernández [b]

[a] Instituto de Ingeniería Mecánica y Producción Industrial, Facultad de Ingeniería, Universidad de la República, 11300 Montevideo, Uruguay
[b] Departamento de Física Aplicada, Universidad de Salamanca, 37008 Salamanca, Spain

ARTICLE INFO

*Article history:*
Received 11 January 2010
Accepted 29 October 2010
Available online 5 November 2010

*Keywords:*
Thermodynamic optimization
Quasi-dimensional simulation
Spark ignition engine
Work losses

ABSTRACT

A quasi-dimensional computer simulation and theoretical methods are applied in order to optimize some design parameters of a realistic spark ignition engine. In particular, we analyze the sensitivity of power output and thermal efficiency to the location of the ignition kernel and to the stroke–bore ratio. Whenever autoignition effects are not considered a centered ignition location returns the highest power output and efficiency (for intermediate and high speeds a centered spark plug leads to power improvements around 10% and efficiency improvements around 2%). It is explicitly shown that this corresponds to the maximum area development of the flame front and to minimum net work losses (including heat transfer, mechanical frictions and working fluid internal irreversibilities). On the other hand, the evolution of maximum power output and maximum efficiency is not linear with the stroke–bore ratio, $R_{sb}$. There is an optimum interval ($R_{sb} \simeq 0.6–0.8$) where it is possible to simultaneously obtain high power outputs and good efficiencies. We have also analyzed the optimum values of stroke–bore ratio that give the best efficiencies for certain intervals of the required power output. For power requirements over 2 kW, $R_{sb}$ around 0.5–1.0 leads to 6% better efficiencies respect to other values.



## 1. Introduction

Two alternative techniques have been used in the last years in order to analyze and optimize internal combustion engines. On one side, it is well-known the versatility of numerical computer simulations based upon the resolution of a set of coupled differential equations arising from the mechanics and the thermodynamics of the engine [1–3]. With the computer hardware nowadays available it is possible: a) to obtain results for the engine performance records matching fairly good with those measured in real engines; b) to check the influence of particular parameters, which testing is neither easy nor cheap in benchmark engines at the lab; and c) to get the most interesting configuration for a certain objective. On the other side, theoretical methods as finite-time thermodynamics allow to analyze the physical basis underlying the engine evolution and to propose optimization methods founded on simple analytical equations depending on the main variables and parameters of control of the system [4–6].

Recently, we have developed and validated a quasi-dimensional computer simulation that includes a realistic chemistry of combustion, the existence of an unburned charge fraction, heat transfers through the cylinder walls, frictions, and a turbulent combustion model with two coupled differential equations for the masses of burned and unburned gases inside the combustion chamber [7]. This simulation scheme leads to good values of power output and efficiency when the simulated results are compared with experiments. Moreover, we have also shown the interest of merging computer simulation possibilities and theoretical thermodynamic optimization in order to obtain the optimum working parameters of the engine for a specific engine design. This includes the optimization of spark advance as a function of the engine speed, the fuel ratio and the cylinder wall temperature. It was introduced an optimization criterion where for a fixed required power output value, the best efficiency of the engine is considered as the objective [8]. It is easy to set up this optimization procedure from power–efficiency implicit plots [9], where the engine speed is the parametric variable, and allow to obtain the optimum distribution of control variables in terms of the engine speed.

The present work constitutes a step forward along our previous results [7,8]. In particular, the goal here is to analyze the sensitivity of a realistic Otto engine on two basic design parameters: the

* Corresponding author. ETSII de Béjar, Universidad de Salamanca, 37700 Béjar, Salamanca, Spain. Tel.: +34 923 29 44 36; fax: +34 923 29 45 84.
*E-mail addresses:* pcurto@fing.edu.uy (P.L. Curto-Risso), amd385@usal.es (A. Medina), anca@usal.es (A. Calvo Hernández).

1359-4311/$ – see front matter © 2010 Elsevier Ltd. All rights reserved.
doi:10.1016/j.applthermaleng.2010.10.029

**Nomenclature**

| | |
|---|---|
| $\eta$ | engine thermal efficiency (fuel conversion efficiency) |
| $\omega$ | engine speed |
| $\rho_b$ | burned gases density |
| $\rho_u$ | unburned gases density |
| $\tau_b$ | characteristic time for the combustion of an eddie of length $l_t$ at an speed $S_l$ |
| $a$ | crankshaft radius |
| $A_f$ | flame front area |
| $B$ | cylinder bore |
| $l_t$ | unburned eddies characteristic length |
| $m_{\text{fuel}}$ | mass of fuel inside the cylinder after closing the intake valve |
| $m_b$ | burned gases mass |
| $m_e$ | total mass inside the flame front |
| $P$ | net power output |
| $Q_{LHV}$ | lower isochoric calorific value of the fuel |
| $r$ | compression ratio |
| $R_c$ | ignition location |
| $R_f$ | radius of the spherical flame front |
| $R_{sb}$ | stroke–bore ratio |
| $S_l$ | laminar burning velocity |
| $t$ | cycle time duration |
| $u_t$ | convective velocity at which the fresh mixture crosses the flame front |
| $V_{\text{cyl}}$ | maximum volume of the combustion chamber |

location of the ignition kernel respect to the cylinder center and the ratio between the length of the stroke and the cylinder bore. By means of the simulations we obtain specific results for the engine power output and thermodynamic efficiency for several values of those parameters and use power–efficiency plots to get their optimum values. Moreover, we investigate the physical origin of the optimal configurations by looking at the work losses. In our model these losses are accounted for three terms: one associated to the heat transfers from the fluid to the cylinder walls, another one linked to the mechanical frictions between the piston and the cylinder and a third one that compiles all fluid internal irreversibilities [10,11].

Recent research work on spark ignition engines is focused on three basic fields [12]: investigation of alternatives for the prevailing fuels (gasoline), to modify the existing designs and operation regimes for gasoline engines in order to improve output records or decrease emissions, and to consider modified designs with alternative fuels. This work directly refers to the second area. We show that the analysis of two basic design parameters (spark plug position and stroke–bore ratio) leads to important improvements on performance output records as power and thermal efficiency. In the case of the spark plug position, centered ignition for high-octane fuels enhances power up to 10% and efficiency 2%. Four-stroke engine designers are always concerned with the question of optimum stroke–bore ratios [3], because it directly affects friction and heat transfer losses, and so, fuel economy. We shall show that maximum power output and maximum efficiency have a maximum as functions of the stroke–bore ratio $R_{sb}$, and it is possible to find an interval for $R_{sb}$ that gives concomitant high values for both power and efficiency. Moreover, we deep in the physical basis of those results in terms of work losses.

## 2. Quasi-dimensional engine model

We consider as control volume the region inside the cylindrical combustion chamber and set up the first principle of thermodynamics separately for unburned ($u$) and burned ($b$) gases, *i.e.*, we assume a two-zone combustion model. Except during combustion the working fluid is an adiabatic mixture of ideal gases with temperature and pressure independent gas constants. The fuel ratio is also constant and the enthalpy changes (except in combustion) are only associated to temperature variations. All these considerations allow to formulate a set of coupled differential equations for the temperature and the pressure inside the cylinder (equations are explicitly given in Sec. II of Ref. [7]).

The solution of this set of coupled equations requires the model of the four strokes during the engine evolution, in particular models for intake and exhaust processes (gases flows through the valves, including overlapping), heat transfers from the working fluid to the cylinder walls, piston frictions, and a detailed analysis of the chemical reactions (see Sec. II of Ref. [8]).

Respect to the combustion process (see Sec. II.A of Ref. [8]), we consider two different control volumes separated by the flame front, one formed by the unburned gases and the other made up by the burned gases. Chemical variations of enthalpy, as well as, those coming from temperature changes are incorporated. The initial burned gases temperature is calculated as an adiabatic flame temperature [2] at constant pressure. The evolution of unburned and burned gas masses during combustion is calculated from the quasi-dimensional model proposed by Blizard and Keck [14,15]. Turbulence is modeled by considering unburned eddies inside the flame front during flame propagation. Those eddies have a characteristic length, $l_t$. The fresh mixture crosses the flame front at a characteristic convective velocity, $u_t$. Time evolution of masses is obtained from a set of coupled differential equations for the burned gases mass, $m_b$, and for the total mass inside the flame front (including burned gases and unburned eddies), $m_e$:

$$\dot{m}_b = A_f \rho_u S_l + \frac{m_e - m_b}{\tau_b} \tag{1}$$

$$\dot{m}_e = A_f \rho_u \left[ S_l + u_t \left( 1 - e^{-t/\tau_b} \right) \right] \tag{2}$$

where $A_f$ is the area of the flame front supposed spherical (see the Appendix for a detailed description on its calculation). Burned gases mass rate has two contributions, the term $A_f \rho_u S_l$, where $S_l$ is the laminar burning velocity, comes from the laminar propagation forward of the flame front and the second addend $(m_e - m_b)/\tau_b$ comes from the burning of the entrained gases. It is considered that the combustion of an eddy of typical length $l_t$ at a speed $S_l$ requires a characteristic time $\tau_b = l_t/S_l$ [2]. Equation (2) gives the time evolution of the total mass inside the flame front. At short times the laminar burning velocity is predominant and for $t >> \tau_b$ the evolution rate is associated to $S_l + u_t$. During the duration of combustion this set of coupled differential equations is also coupled with the differential equations governing the evolution of temperatures and pressure. These equations are explicitly written in [7].

The results of our simulation model, including the mentioned combustion model, were validated in [7,16] by comparing computational results with the experiments by Beretta *et al.* [17]. It was shown a fair agreement between experimental and simulated pressure, and also good comparisons for the evolution of the fraction of burned gases and the area of the flame front as functions of the crankshaft angle. This essentially means that the elected combustion model is adequate to account for both power output and efficiency.

We follow the procedure developed in Refs. [7,8] to calculate the net power output of the engine and its thermal efficiency. Work losses are evaluated within finite-time-thermodynamics scheme [6,10,18]. Briefly, a simple analytical model for an Otto cycle including the main irreversibility sources is proposed, and the comparison of the predictions of such model with simulation results provide numerical information, for instance, of the work losses during the engine evolution [7]. The net power output, $P = |W|/t$, where $t$ is the cycle time duration, incorporates work losses associated to internal irreversibilities, $|W_{\text{int}}|$, heat transfer losses, $|W_Q|$, and work losses arising from the frictions of the piston with the cylinder walls, $|W_{\text{fric}}|$. Thus, the total work losses can be written as:

$$|W_l| = |W_{\text{int}}| + |W_Q| + \left|W_{\text{fric}}\right| \tag{3}$$

The engine efficiency is obtained as

$$\eta = \frac{|W|}{m_{\text{fuel}} Q_{LHV}} \tag{4}$$

where $m_{\text{fuel}}$ is the mass of fuel inside the cylinder after closing the intake valve and $Q_{LHV}$ is the lower isochoric calorific value of the fuel [3]. This definition of engine efficiency is fuel conversion efficiency, because $m_{\text{fuel}}Q_{LHV}$ is the chemical energy which can be released by the combustion of the fuel mass per cycle [2,19].

All the results we present were obtained for the reference fuel for Otto based engines, iso-octane, $C_8H_{18}$. We considered the unburned gas mixture composed by fuel, air, and residual gases. The program CEA developed by NASA [20] was employed to solve combustion and to calculate the composition of exhaust. All the chemical species were considered as ideal gases, and the corresponding constant pressure specific heats were taken as seven parameter temperature polynomials [20]. The thermodynamic system of differential equations as well as the equations for the evolution of masses during combustion were solved by means or a 4th-order Runge-Kutta algorithm. Table 1 contains a summary of the main geometrical and configuration parameters required to run the simulations. More details on other parameters and on the validation of the simulation can be found in Refs. [7,8].

## 3. Influence of geometrical parameters of the combustion chamber on engine performance records

### 3.1. Ignition location

Ignition location, $R_c$, (see Figs. 1 and 2) is the distance between the cylinder center and the position of the ignition kernel, where combustion begins its development. When turbulence or fluctuations of the mixture around the spark plug are not considered, $R_c$ represents the spark plug position. We include in the Appendix a detailed description of the flame front volume growth (considered as spherical) and its relation with the flame front area, $A_f$, through geometrical relations. This is used in the simulation to calculate the evolution of mass of burned gases by means of Eqs. (1) and (2). It is clear the strong dependence of the flame front area with $R_c$, and thus, of the evolution of the mass of gases. As $R_c$ approaches the cylinder radius, the flame front earlier reaches the cylinder wall, and thus its area is reduced. When $R_c$ approaches zero, *i.e.*, the spark plug is located close to the cylinder center, the flame front spends some more time to reach the walls and so it develops with a larger area.

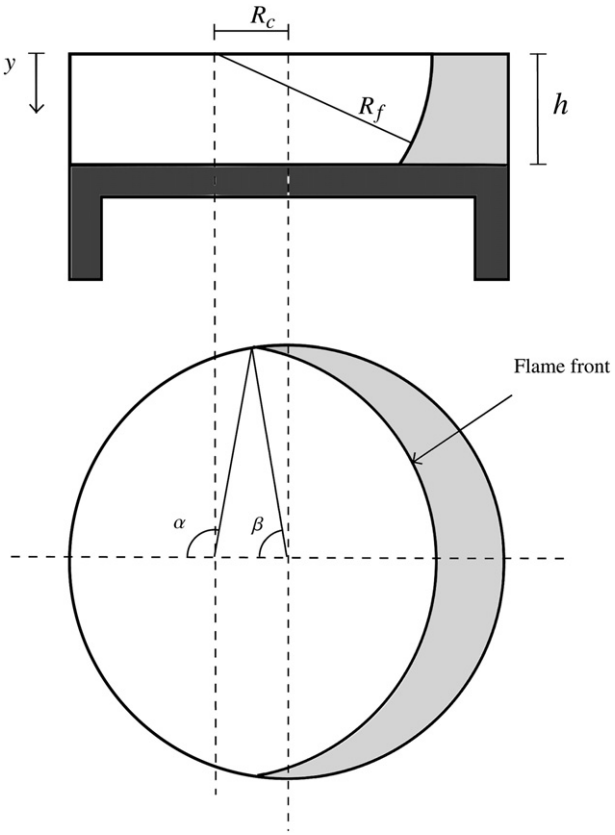


**Fig. 1.** Geometrical definitions for the calculation of the flame front area in the case of a non-centered ignition location.

**Table 1**
Some parameters required to run the numerical simulations.

| | |
|---|---|
| $V_{\text{cyl}}$, cylinder volume | $8.0 \times 10^{-4}$ m$^3$ |
| $a$, crank radius | $4.8 \times 10^{-2}$ m |
| $B$, piston bore | $9.6 \times 10^{-2}$ m |
| $R_{sb}$, stroke–bore ratio | 1 |
| $R_c$, spark-plug position | 0 |
| $r$, compression ratio | 8 |
| $\mu$, friction coefficient | 16.0 kg/s |
| $p_{\text{in}}$, intake pressure | $0.75 \times 10^5$ Pa |
| $T_{\text{in}}$, intake temperature | 350.0 K |
| $p_{\text{ex}}$, external pressure at exhaust | $1.05 \times 10^5$ Pa |
| $T_w$, cylinder internal wall temperature | 500 K |
| $\phi_0$, spark advance | 330° |
| $\varphi$, fuel–air equivalence ratio | 1 |

Fig. 3 shows the results for the power output $P(\omega)$ and the efficiency $\eta(\omega)$ from our simulations for an speed interval $\omega$ between 20 and 400 rad/s and three values of $R_c$: 0 (centered spark plug), 10 mm and 20 mm. From Fig. 3(a) we see that at intermediate and high speeds, power output increases as $R_c$ trends to zero with a right shifting of the corresponding maximum value. For low speeds ($\omega \lesssim 75$ rad/s) the behavior of power output with $R_c$ is opposite and then larger $R_c$ values lead to larger power output, although these numerical differences are quite small, as can be seen from a closer inspection of the lower left corner in Fig. 3(a).

The evolution of the engine efficiency with the ignition location is depicted in Fig. 3(b). Similarly to power output, above $w \simeq 100$ rad/s, higher efficiencies are obtained as $R_c$ decreases, while for very small speeds the evolution of efficiency with $R_c$ is reversed: higher $R_c$ gives higher efficiencies, but numerical differences are small. The similar behavior of $P(\omega)$ and $\eta(\omega)$ with $R_c$ observed in Fig. 3 can be explained because of the relationship between power and efficiency is the chemical energy that enters to the system through the fuel (Eq. (4)), which is independent of the

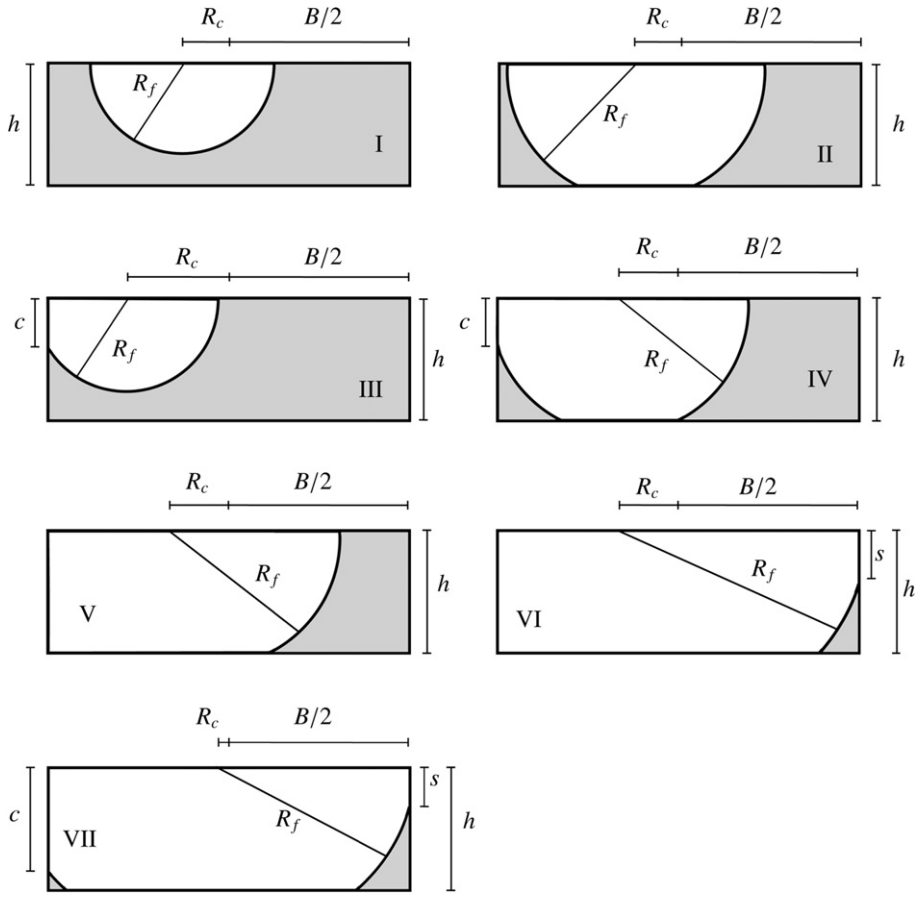


**Fig. 2.** Possible flame front configurations for a non-centered ignition location.

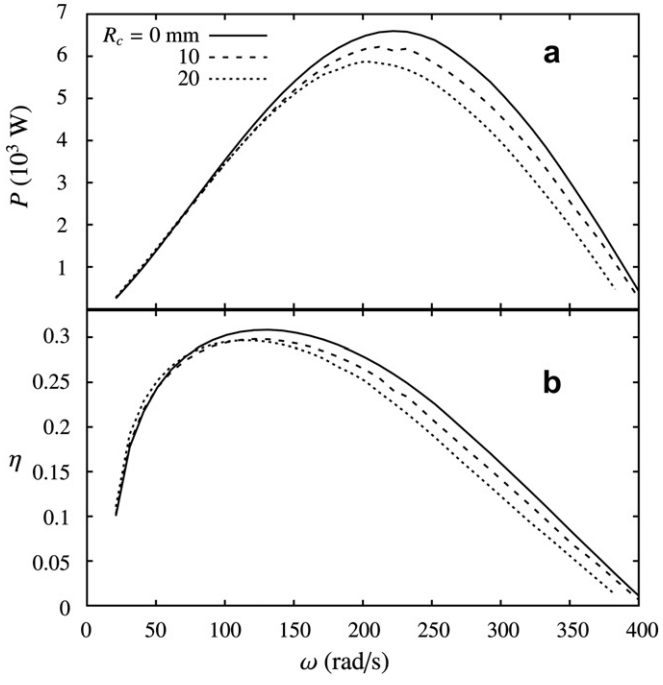


**Fig. 3.** (a) Power output of the simulated engine for several values of the ignition location, $R_c$. (b) Efficiency of the engine for the same parameters.

spark plug position $R_c$. In Fig. 4 we represent the simultaneous evolution of power output and efficiency by parametric elimination of the speed between the curves $P = P(\omega)$ and $\eta = \eta(\omega)$.

It is clear from the results in Figs. 3 and 4 that a centered spark plug position $R_c = 0$ returns better values both for maximum power and maximum efficiency. For low speeds the consideration of high values of $R_c$ does not improve neither power output nor efficiency, but for intermediate and high speeds a centered spark plug position lead to power improvements around 10% and efficiency improvements around 2%. From a physical viewpoint this could be associated to the size of the flame front area, that is larger for a centered spark (see the Appendix and Fig. 2). Thus, the exchange area is larger and the combustion speed increases. It is remarkable that

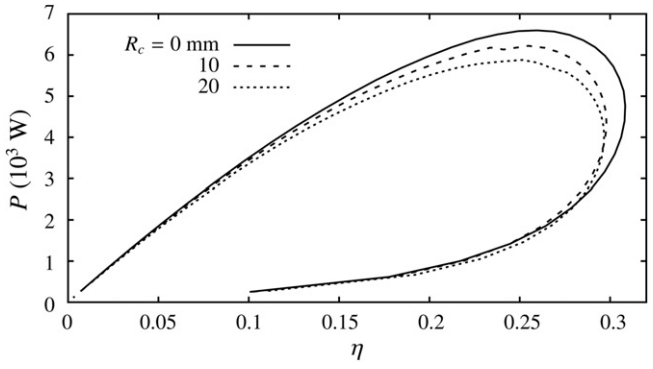


**Fig. 4.** Power–efficiency curves for the labeled values of the ignition location.

this increment on combustion speed involves an increase of the pressure inside the chamber that eventually could exceed fuel autoignition limits. Some authors [13] mention such reason to justify that sometimes in real car engines the spark plug position is not centered in the cylinder. Our simulation does not include autoignition effects, so our analysis should be considered only for fuels with high enough octane number.

It is elucidating to analyze the influence of the spark plug position from the complementary point of view of the work losses, instead of investigating its influence on the power and efficiency. In Fig. 5 we show the work losses associated to heat transfers through cylinder walls, $|W_Q|$, frictions, $|W_{fric}|$, and internal irreversibilities, $|W_{int}|$, as well as the net work losses, $|W_l|$ (Eq. (3)). From this figure we note that:

i) Heat transfer, $|W_Q|$, and internal, $|W_{int}|$, losses show at intermediate speeds (100–250 rad/s) a clear dependence on $R_c$ while they become practically $R_c$-independent at low and high speeds.
ii) Friction losses, $|W_{fric}|$, are independent of $R_c$, and according with the friction model we elected [7], linearly depend on $\omega$.
iii) At low speeds net losses, $|W_l|$, are essentially due to heat transfers, but at intermediate and high speeds internal losses are dominant. So, $|W_l|$ rapidly decreases as it does $|W_Q|$, reach a minimum (approximately when $|W_{int}|$ becomes dominant) and then increases with $\omega$. The smallest total work losses, in all the speed range, are obtained with the centered ignition location, and for approximately $\omega = 130$ rad/s reaches its minimum value.
iv) Indeed, at intermediate speeds net losses increase as $R_c$ increases, in agreement with the decreasing observed for the power and efficiency in Figs. 3 and 4.

### 3.2. Stroke–bore ratio

The stroke–bore ratio is the rate between the stroke (twice the crankshaft radius, $a$) and the cylinder bore, $B$, $R_{sb} = 2a/B$. Large bore to stroke ratio (*oversquare* engines, $R_{sb} < 1$) improves induction and exhaust (specially at high speeds) because it admits larger valves, but the combustion chamber has a poor surface-to-volume ratio and in consequence more heat transfer losses [3]. On the contrary piston friction losses are smaller because of the reduced distance travelled by the piston during each engine rotation. Crank stress is also lower due to lower peak piston speed relative to engine speed. This type of design is usually elected to get more peak torque at high speeds. *Undersquare* designs ($R_{sb} > 1$) favors fuel economy because the better surface-to-volume ratio of the combustion chamber, thus recently there has been a return to undersquare engines.

We analyze in this section the influence of $R_{sb}$ on the power output and efficiency, keeping constant the maximum volume of the combustion chamber, $V_{cyl}$, and the compression ratio, $r$. From the geometry of the system it is straightforward to obtain the following relations [2,16]:

$$B = \left[\frac{4(r-1)V_{cyl}}{\pi r R_{sb}}\right]^{1/3} \tag{5}$$

$$a = \left[\frac{(r-1)V_{cyl}}{2\pi r}\right]^{1/3} R_{sb}^{2/3} \tag{6}$$

We consider the values of $V_{cyl}$ and $r$ contained in Table 1 and change $a$ and $B$ to get an interval for $R_{sb}$ between 0.2 and 1.5. Fig. 6 represents the evolution of power output with the speed for four values of $R_{sb}$ in that interval. At low speeds power output is almost independent of $R_{sb}$ but over 100 rad/s the influence of $R_{sb}$ is important: the intermediate values of $R_{sb}$ ($R_{sb} = 0.5$ and 1.0) return high power values, while low or high stroke–bore ratios lead to smaller power output. Comparing maximum power values, the difference between the lowest one (corresponding to $R_{sb} = 0.2$) and the highest one (corresponding to $R_{sb} = 1.0$) is significant, around 18%. The effect of $R_{sb}$ on efficiency, see Fig. 6(b), is similar to that on power output: the intermediate values of $R_{sb}$ give higher maximum efficiencies, although the differences (7% between the outermost values) are smaller than for power output. From the results in Fig. 6, we stress that for any $R_{sb}$-value the speed giving the maximum power output could be considered as the operation limit of the

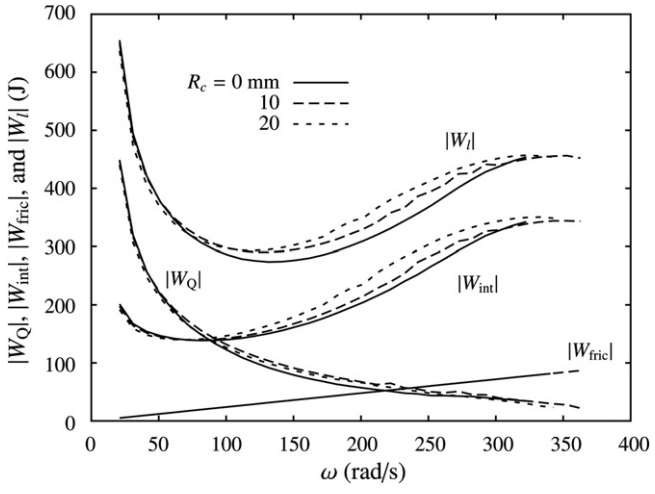


**Fig. 5.** Work losses as a function of its rotational speed, considering the ignition location $R_c$ as control parameter. $|W_Q|$, work losses associated to heat transfers through the cylinder walls; $|W_{int}|$, work losses associated to internal irreversibilities; $|W_{fric}|$, work losses associated to piston frictions; and $|W_l|$, net work losses.

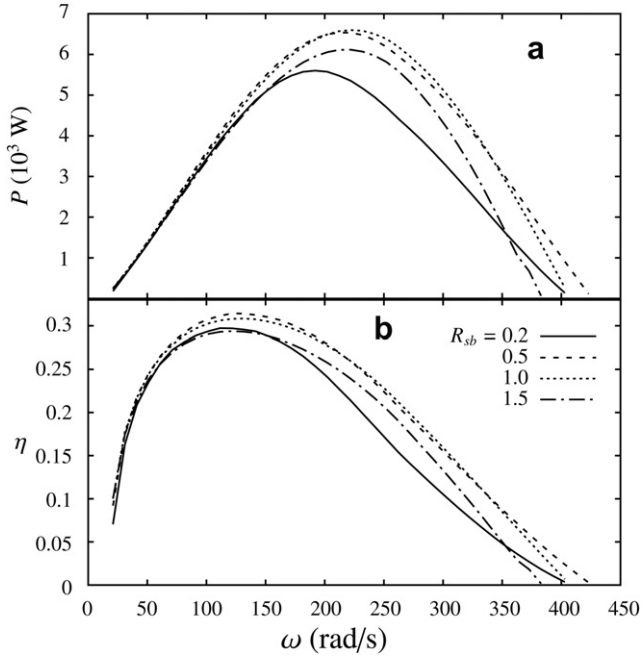


**Fig. 6.** (a) Power output of the simulated engine for several values of the stroke–bore ratio, $R_{sb}$, and fixed values of the maximum volume of the chamber and the compression ratio. (b) Efficiency of the engine for the same parameters.

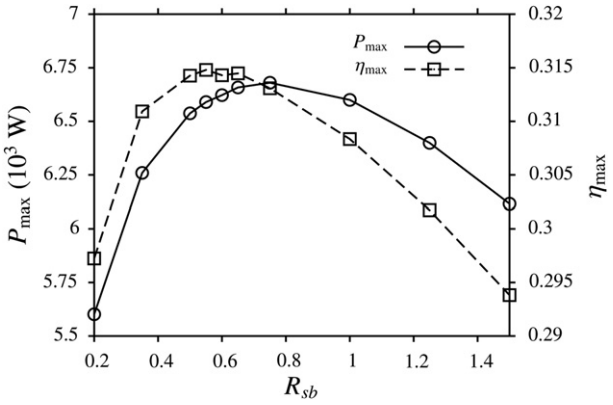


**Fig. 7.** Maximum values of the power output, $P_{max}$, and the efficiency, $\eta_{max}$, in terms of the stroke–bore ratio, $R_{sb}$.

engine, because for any speed over this one it is always possible to find another speed giving the same power but a better efficiency.

We have run additional simulations for several values of $R_{sb}$, between 0.2 and 1.5, in order to analyze the possible non-linear behavior of the maximum values of power output and efficiency in terms of $R_{sb}$, as suggested by Fig. 6. Accordingly, in Fig. 7 we represent the dependence of the maximum values of power output, $P_{max}$, and efficiency, $\eta_{max}$, on $R_{sb}$. Actually, the evolution of both maxima is not linear: the curves have a maximum, which for power is around $R_{sb} = 0.8$ and for efficiency is around 0.6. Within the interval [0.6, 0.8] it is possible to find simultaneously high values of $P_{max}$ and $\eta_{max}$. It would constitute the optimal working interval for this parameter when the objective is to get good values of $P_{max}$ and $\eta_{max}$, independently of the speed.

Taking into account that in a real engine power requirements change during its utilization, a different objective or optimization criterion is to obtain the maximum efficiency for a required power output [8]. Power–efficiency curves allow for a direct application of this criterion. As it is shown in Fig. 8, when the required power is below approximately 2 kW, whichever small or high values give very similar efficiencies, but for higher power requirements $R_{sb}$ around 0.5–1.0 leads to better efficiencies (up to 6% respect to $R_{sb} = 1.5$).

To deep in the physical origin of the interesting behavior of power and efficiency in terms of $R_{sb}$ we plot in Fig. 9 the evolution of work losses with the engine speed for some values of $R_{sb}$. The differences among work losses associated to heat transfers through cylinder walls, $|W_Q|$, are only appreciable for speeds under 150 rad/s. Something different happens for fluid internal losses, $|W_{int}|$, where differences are important from 100 rad/s. As commented by Descieux *et al.* [9], the larger the stroke compared to the bore, the

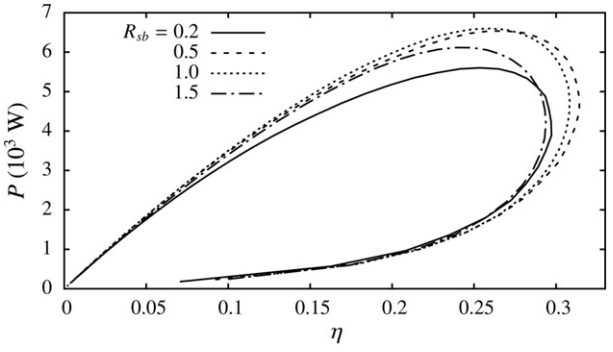


**Fig. 8.** Power–efficiency curves for several values of the stroke–bore ratio, $R_{sb}$.

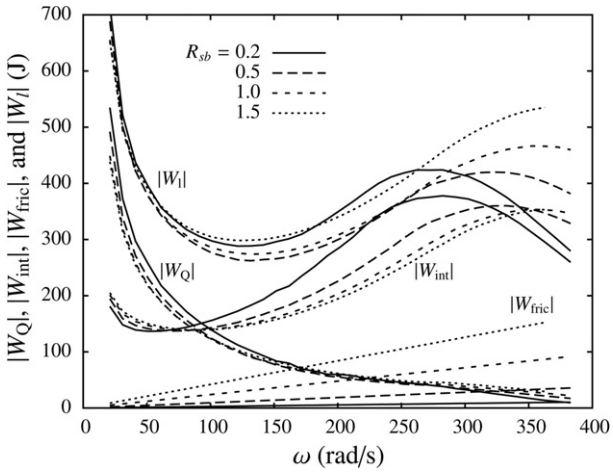


**Fig. 9.** Work losses as a function of the stroke–bore ratio. Notation as in Fig. 3.

larger the mean velocity of the piston, and then friction losses, $|W_{fric}|$. Fig. 9 shows the expected results for friction losses: for a given $R_{sb}$ they linearly increase with $\omega$, and for a fixed $\omega$ linearly increase with $R_{sb}$. Respect to heat transfer losses $|W_Q|$, as $R_{sb}$ decreases the combustion chamber has a poorer surface-to-volume ratio, so heat transfer losses increase. This is observed in Fig. 9 specially when heat transfer losses are more relevant, *i.e.*, at low speeds. The joint influence of these factors lead to the minimization of the net work losses $|W_I|$ in almost all the speeds interval for $R_{sb}$-values around 0.5–1.0. This corroborates the optimal election of this parameter as we discussed before.

From another perspective, recently Ozcan *et al.* [12] have analyzed the performance and emission characteristics of an LPG powered four-stroke spark ignition engine under variable stroke length (and so, variable compression ratio). In fixed stroke engines the load variation is balanced by throttling the intake fuel–air mixture, so friction losses remain constant, while in variable stroke engines these losses are reduced: a short stroke is used for low engine load and longer strokes are used for high engine loads. Their simulations report brake torque and power increases about 7–54% respect to the original design. The results of our calculations are interesting from the viewpoint of the design of fixed stroke engines, since our simulations estimate stroke–bore intervals leading to a good compromise between power output and thermal efficiency.

## 4. Summary and conclusions

We have simulated the power output and the efficiency of a realistic Otto-like engine by means of a quasi-dimensional simulation incorporating a turbulent combustion model. The simulation includes a scheme to introduce the influence of the ignition location, *i.e.*, the distance from the cylinder center at which ignition kernel develops. Provided that autoignition effects are not considered, centered ignition gives the highest power output and efficiency, while the consideration of high values of $R_c$ does not improve neither power output nor efficiency. Physically this is associated to the larger size of the flame front area for a centered spark and to the fact that total work losses in such situation are minimized. Total work losses in our calculations include losses associated to heat transfers through cylinder walls, frictions between the piston and the walls and internal irreversibilities in the dynamics of the fluid itself.

We have also analyzed the sensitivity of engine output parameters to the stroke–bore ratio, $R_{sb}$. Looking for the maximum

values of power output and efficiency, intermediate values between 0.6 and 0.8 give the most favorable results (about 18% better for power output and 7% better for efficiency) than those obtained with too low or too high stroke–bore ratios. Another optimization procedure can look to obtain the better efficiency for a required value of power output. This procedure is easily associated to the power–efficiency curves obtained by eliminating the engine speed. For required power outputs below 2 kW, any value of $R_{sb}$ give similar efficiencies, but when the required power is higher $R_{sb}$ around 0.5–1.0 leads to better efficiencies. Work losses plots clearly show that these optimum values of $R_{sb}$ minimize net work losses in a wide speed interval.

In summary, this work provides a computer simulation method to predict optimum values of two basic parameters that concerns any four-stroke spark ignition engine designer, the location of ignition kernel and the stroke to bore ratio. Moreover, the merging of the capabilities of computer simulations and theoretical schemes allow to deep in the physical foundations of those optimum values in terms of work losses.

## Acknowledgements

We acknowledge financial support from *Ministerio de Educación y Ciencia* of Spain under Grant FIS2010-17147 and also from *Junta de Castilla y León* under Grant SA054A08.

## Appendix

In order to solve the Eqs. (1) and (2) for combustion it is necessary to know the flame front area, $A_f$, during the combustion process. Assuming a spherical flame front, $A_f$, can be calculated from its radius, $r_f$. In the literature several methods can be found, based either on empirical relations for $R_f$ [17], or on the computation of the volume of burned gases during combustion [21]. We follow the last one considering that the volume of gases inside the flame front, $V_b$, can be expressed as:

$$V_f = V_b + \frac{m_e - m_b}{\rho_u} \tag{7}$$

where $V_b = m_b/\rho_b$.

Also there exist in the literature approximate iterative procedures to estimate the flame front area when $R_c \neq 0$ [14,22]. Nevertheless, we follow an exact procedure distinguishing seven possible flame front configurations during the evolution of combustion. We denote $A_c$ the area of a horizontal section of the volume of gases inside the flame front at a vertical position $y$ in the cylinder and $P_c$ is the perimeter of that section:

$$A_c\left(R_f, R_c, B, y\right) = \frac{\beta B^2}{4} + \left(R_f^2 - y^2\right)(\pi - \alpha) - \frac{R_c B}{2}\sin\beta \tag{8}$$

$$P_c\left(R_f, R_c, B, y\right) = 2(\pi - \alpha)\sqrt{R_f^2 - y^2} \tag{9}$$

where the angles $\alpha$ and $\beta$ (see Fig. 1) are obtained through the following geometrical relations:

$$\alpha\left(R_f, R_c, B, y\right) = \arccos\left[\frac{B^2 - 4\left(R_f^2 - y^2 + R_c^2\right)}{8R_c\sqrt{R_f^2 - y^2}}\right] \tag{10}$$

$$\beta\left(R_f, R_c, B, y\right) = \arccos\left[\frac{B^2 - 4\left(R_f^2 - y^2 - R_c^2\right)}{4R_c B}\right] \tag{11}$$

In the Figs. 2 and 7 possible cases throughout the flame front evolution are specified:

- Case I:

$$V_f = \frac{2}{3}\pi R_f^3 \tag{12}$$

$$R_f = \left(\frac{3V_f}{2\pi}\right)^{1/3} \tag{13}$$

$$A_f = 2\pi R_f^2 \tag{14}$$

- Case II:

$$V_f = \frac{\pi}{3}h\left(3R_f^2 - h^2\right) \tag{15}$$

$$R_f = \sqrt{\frac{1}{3}\left(\frac{3V_f}{h\pi} + h^2\right)} \tag{16}$$

$$A_f = 2\pi R_f h \tag{17}$$

- Case III:

$$V_f = \int_0^c A_c\left(R_f, R_c, B, y\right)\mathrm{d}y + \int_c^{R_f} \pi\left(R_f^2 - y^2\right)\mathrm{d}y \tag{18}$$

$$A_f = \int_0^c P_c\left(R_f, R_c, B, y\right)\mathrm{d}y + \int_c^{R_f} 2\pi\sqrt{R_f^2 - y^2}\,\mathrm{d}y \tag{19}$$

- Case IV:

$$V_f = \int_0^c A_c\left(R_f, R_c, B, y\right)\mathrm{d}y + \int_c^{h} \pi\left(R_f^2 - y^2\right)\mathrm{d}y \tag{20}$$

$$A_f = \int_0^c P_c\left(R_f, R_c, B, y\right)\mathrm{d}y + \int_c^{h} 2\pi\sqrt{R_f^2 - y^2}\,\mathrm{d}y \tag{21}$$

- Case V:

$$V_f = \int_0^h A_c\left(R_f, R_c, B, y\right)\mathrm{d}y \tag{22}$$

$$A_f = \int_0^h P_c\left(R_f, R_c, B, y\right)\mathrm{d}y \tag{23}$$

- Case VI:

$$V_f = \frac{s\pi B^2}{4} + \int_s^h A_c\left(R_f, R_c, B, y\right)\mathrm{d}y \tag{24}$$

$$A_f = \int_s^h P_c\left(R_f, R_c, B, y\right)\mathrm{d}y \tag{25}$$

- Case VII:

$$V_f = \frac{s\pi B^2}{4} + \int_s^c A_c\left(R_f, R_c, B, y\right)\mathrm{d}y + \int_c^h \pi\left(R_f^2 - y^2\right)\mathrm{d}y \tag{26}$$

$$A_f = \int_s^c P_c\left(R_f, R_c, B, y\right)\mathrm{d}y + \int_c^h 2\pi\sqrt{R_f^2 - y^2}\,\mathrm{d}y \tag{27}$$

$s$ and $c$ are the heights of the intersections of the flame front with the cylinder walls (see Fig. 2). The particular case of a centered ignition location is direct by performing in each case the limit $R_c \to 0$.

It is worth mentioning that the same kind of analysis is necessary in order to get a proper description of heat transfers from the working fluid to the cylinder walls. During combustion heat transfer calculations are divided into two parts associated either to unburned or burned gases, each one with its own temperature. Details can be found in Ref. [16].

## References


[1] C.R. Ferguson, Internal Combustion Engines, Applied Thermosciences. John Wiley & Sons., 1986.
[2] J.B. Heywood, Internal Combustion Engine Fundamentals. McGraw-Hill, 1988.
[3] R. Stone, Introduction to Internal Combustion Engines. Macmillan Press LTD, 1999.
[4] A. Bejan, E. Mamut, Thermodynamic Optimization of Complex Energy Systems, In: NATO Science Series. Kluwer Academic, 1999.
[5] R.S. Berry, V. Kazakov, S. Sieniutycz, Z. Szwast, A.M. Tsirlin, Thermodynamic Optimization of Finite-Time Processes. Wiley, 2000.
[6] A. Fischer, K.H. Hoffmann, Can a quantitative simulation of an Otto engine be accurately rendered by a simple Novikov model with heat leak? J. Non-Equilib. Thermodyn. 29 (2004) 9–28.
[7] P.L. Curto-Risso, A. Medina, A. Calvo Hernández, Theoretical and simulated models for an irreversible Otto cycle, J. Appl. Phys. 104 (2008) 094911.
[8] P.L. Curto-Risso, A. Medina, A. Calvo Hernández, Optimizing the operation of an spark ignition engine: simulation and theoretical tools, J. Appl. Phys. 105 (2009) 094904.
[9] D. Descieux, M. Feidt, One zone thermodynamic model simulation of an ignition compression engine, Appl. Therm. Eng. 27 (2007) 1457–1466.
[10] F. Angulo-Brown, J.A. Rocha-Martínez, T.D. Navarrete-González, A non-endoreversible Otto cycle model: improving power output and efficiency, J. Phys. D: Appl. Phys. 29 (1996) 80–83.
[11] F. Angulo-Brown, T.D. Navarrete-González, J.A. Rocha-Martínez, An irreversible Otto cycle model including chemical reactions. in: C. Wu, L. Chen, J. Chen (Eds.), Recent Advances in Finite-Time Thermodynamics. Nova Science Publishers, Commack, New York, 1999.
[12] H. Özcan, J. Yamin, Performance and emission characteristics of lpg powered four stroke si engine under variable stroke length and compression ratio, Energy Convers. Manage. 49 (2008) 1193–1201.
[13] C.F. Taylor, The Internal Combustion Engine in Theory and Practice. The Massachusetts Institute of Technology, 1985.
[14] N.C. Blizard, J.C. Keck, Experimental and theoretical investigation of turbulent burning model for internal combustion engines, SAE(1974) Paper No. 740191.
[15] J.C. Keck, Turbulent flame structure and speed in spark ignition engines, in: Proceedings of Nineteenth Symposium (International) on Combustion. The Combustion Institute, Pittsburgh, 1982, pp. 1451–1466.
[16] P. Curto-Risso, Numerical simulation and theoretical model of an irreversible otto cycle. Ph.D. thesis, Universidad de Salamanca, Spain, http://campus.usal.es/gtfe/ (2009).
[17] G.P. Beretta, M. Rashidi, J.C. Keck, Turbulent flame propagation and combustion in spark ignition engines, Combust. Flame 52 (1983) 217–245.
[18] A. Calvo Hernández, J.M.M. Roco, A. Medina, S. Velasco, An irreversible and optimized four stroke cycle model for automotive engines, Eur. J. Phys. 17 (1996) 11–18.
[19] J.R. Senft, Mechanical Efficiency of Heat Engines. Cambridge University Press, 2007.
[20] B.J. McBride, G. Sanford, Computer Program for Calculation of Complex Chemical Equilibrium Compositions and Applications, Users Manual 1311. National Aeronautics and Space Administration, NASA, June 1996. http://www.grc.nasa.gov/WWW/CEAWeb/.
[21] H. Bayraktar, O. Durgun, Mathematical modeling of spark-ignition engine cycles, Energy Sources 25 (2003) 439–455.
[22] H. Bayraktar, Theoretical investigation of flame propagation process in an SI engine running on gasoline–ethanol blends, Renew. Energy 32 (2007) 758–771.